Carbon dioxide sequestration in deep-sea basalt

David S. Goldberg*, Taro Takahashi, and Angela L. Slagle

Lamont–Doherty Earth Observatory, 61 Route 9W, Palisades, NY 10964

Communicated by Wallace S. Broecker, Lamont–Doherty Earth Observatory of Columbia University, Palisades, NY, May 7, 2008 (received for review April 3, 2008)

Developing a method for secure sequestration of anthropogenic carbon dioxide in geological formations is one of our most pressing global scientific problems. Injection into deep-sea basalt formations provides unique and significant advantages over other potential geological storage options, including (*i*) vast reservoir capacities sufficient to accommodate centuries-long U.S. production of fossil fuel CO_2 at locations within pipeline distances to populated areas and CO_2 sources along the U.S. west coast; (*ii*) sufficiently closed water-rock circulation pathways for the chemical reaction of CO_2 with basalt to produce stable and nontoxic (Ca^{2+}, Mg^{2+}, Fe^{2+})CO_3 infilling minerals, and (*iii*) significant risk reduction for post-injection leakage by geological, gravitational, and hydrate-trapping mechanisms. CO_2 sequestration in established sediment-covered basalt aquifers on the Juan de Fuca plate offer promising locations to securely accommodate more than a century of future U.S. emissions, warranting energized scientific research, technological assessment, and economic evaluation to establish a viable pilot injection program in the future.

climate change | ocean crust | climate mitigation | fossil fuel emissions | energy

In recent years, the debate over the most effective means to stabilize greenhouse gas concentrations in the atmosphere has not focused on a single solution but has endorsed multiple approaches to this global problem that require a variety of technologies (1–4). In its latest report on carbon capture and storage, the Intergovernmental Panel on Climate Change (5) noted that geological storage of industrial CO_2 emissions can contribute significantly to achieving a stable solution over the next several decades. Among geological storage techniques, CO_2 injection into deep saline aquifers, or its reinjection into depleted oil and gas reservoirs, has potentially large storage capacity and geographic ubiquity (6–10). The effectiveness of these methods for CO_2 sequestration depends strongly on the reservoir capacity, retention time, stability, and risk for leakage (11, 12). Gunter *et al.* (13) discuss two primary trapping mechanisms for CO_2 injected into an aquifer: physical trapping and geochemical trapping. The first involves low-permeability caprocks or stratigraphic seals that physically impede vertical migration of injected CO_2 to the surface. Sedimentary aquifers, such as depleted oil reservoirs, offer established reservoirs for physical trapping, but generally lack geochemical trapping potential. Geochemical trapping (13), also known as mineral trapping, involves long-term reactions of CO_2 with host rocks and the formation of stable minerals such as carbonates under *in situ* conditions. In nature, mineral carbonization of host rocks occurs in a variety of well documented settings, such as hydrothermal alteration at volcanic springs (14), through surface weathering (15), and in deep ocean vent systems (16). These processes are commonly associated with serpentinization in ultramafic and mafic rocks exposed to seawater, the breakdown of silicates into clays, and the precipitation of carbonates. Seifritz (17) initially proposed the concept that Mg^{2+} and Ca^{2+} silicates undergoing these processes would be particularly suitable for the stable disposal of CO_2.

Deep-Sea Basalt and CO_2

Deep-sea basalt offers a unique environment for CO_2 sequestration that combines both vast volumes of seawater-filled pore space and Mg-Ca silicate rocks (18). Within deep-sea basalt aquifers, the injected CO_2 mixes with seawater and reacts with basalt, both of which are rich in alkaline-earth elements. The release of Ca^{2+} and Mg^{2+} ions from basalt will form stable carbonate minerals as reaction products (19, 20). Takahashi *et al.* (21) present a general geochemical model for mineral trapping in basalt. Recent laboratory experiments demonstrate the potential for rapid carbonate precipitation in fresh continental flood basalt (22). Dissolution and precipitation reactions in deep-sea basalt can proceed in fluid-filled fractures and pores at rates equal to or greater than measured in the laboratory (22, 23). Carbonate precipitation over time may alter *in situ* porosity and permeability within basalt aquifers, however, and thus progressively decrease the CO_2-basalt reaction rate to a finite limit. Although natural weathering processes in deep-sea basalt precipitate pore-filling carbonates, fractured and permeable basalt crust extends for millions of years before its porosity has been appreciably filled (24). Land-based experiments provide some insight into these effects, but estimating the *in situ* rates and accelerated effects, if any, of carbonate precipitation in basalt are difficult to predict without deep-sea CO_2 injection experiments. Matter *et al.* (25) conducted a small-scale injection experiment in mafic rocks to investigate the *in situ* rates of reaction. Two processes, mixing between the injected solution and aquifer water and the release of cations from water-rock

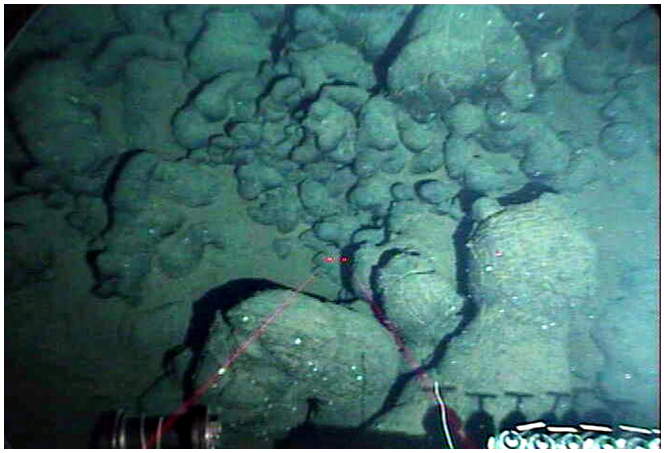

Fig. 1. Deep-sea basalt on the seafloor. Photograph of deep-sea pillow lavas emplaced on the ocean bottom near the Juan de Fuca ridge (data from cruise AT11-16, Alvin Dive 4045; http://4dgeo.whoi.edu). Rounded, intact pillow lavas transition to small cobbles and fragments across the area, forming large interpillow voids. Image scale is ≈1.5 m × 1 m (red laser points are 4 cm apart; water depth is ≈2,200 m).

Author contributions: D.S.G. designed research; D.S.G., T.T., and A.L.S. performed research; T.T. contributed new reagents/analytic tools; A.L.S. analyzed data; and D.S.G. wrote the paper.

The authors declare no conflict of interest.

Freely available online through the PNAS open access option.

*To whom correspondence should be addressed. E-mail: goldberg@ldeo.columbia.edu.

© 2008 by The National Academy of Sciences of the USA

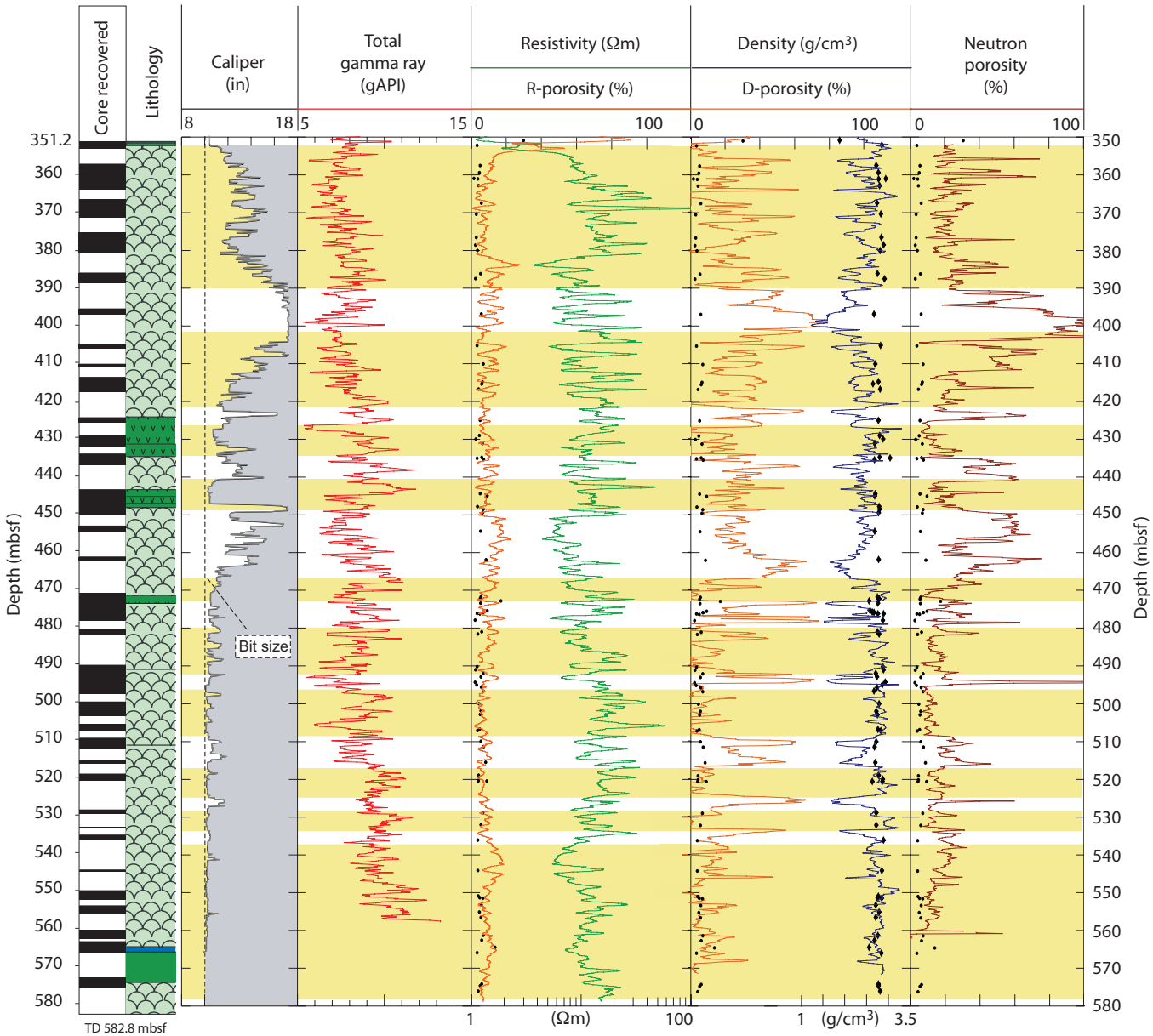

Fig. 2. *In situ* physical properties of basalt below the seafloor. Geophysical log profiles from 350 to 580 m below the seafloor at Site U1301 indicate massive flow layers (yellow) and fractured pillow lava intervals (white). Porosity profiles are computed by using *in situ* electrical resistivity, density, and neutron logs and established relationships for young ocean basalt (42, 43); black dots represent shipboard measurements on core samples (32). *In situ* and core porosity estimates agree in massive flows, but differ in fractured zones because of the enlarged borehole diameter. Core and downhole data come from the Integrated Ocean Drilling Program database (http://www.iodp.org/).

dissolution, were found to neutralize the introduced carbonic acid within 200 h of injection (25). Long residence periods for fluids in the ocean crust (e.g., >500 years) would therefore provide 10^4-fold longer times for dissolution of basalt and release of Ca^{2+} and Mg^{2+} ions from the formation of carbonate minerals.

Important mechanisms for trapping CO_2 injected within deep-sea basalt also include (*i*) blanketing deep-sea sediments, which form a low-permeability stratigraphic barrier impeding vertical fluid migration; (*ii*) the formation of CO_2 hydrate, which is denser and less soluble than liquid CO_2 in seawater <2°C (26); and (*iii*) gravitational trapping at water depths >2,700 m, where injected CO_2 is denser than typical seawater, causing it to sink (27–29). All three of these mechanisms are simultaneously available within ocean crust, providing independent protective barriers that could safely isolate the oceans, benthic ecosystems, and the atmosphere from leakage of CO_2 escaping from deep-sea basalt aquifers.

Juan de Fuca Plate

The extrusion of molten basalt at volcanic ridges into cold seawater forms rounded brittle pillow lavas, commonly having large voids between lobes and broken into fractured rubble (Fig. 1). These formations are overlain by subsequent volcanism such as massive lavas, and then by deep-sea sediments. This creates buried high-permeability aquifers within the upper 500–600 m of the volcanic basement (30). We propose that such layers are suitable reservoirs for CO_2 injection.

The eastern flanks of the Endeavor and Blanco segments of the Juan de Fuca ridge, situated within a few hundred kilometers

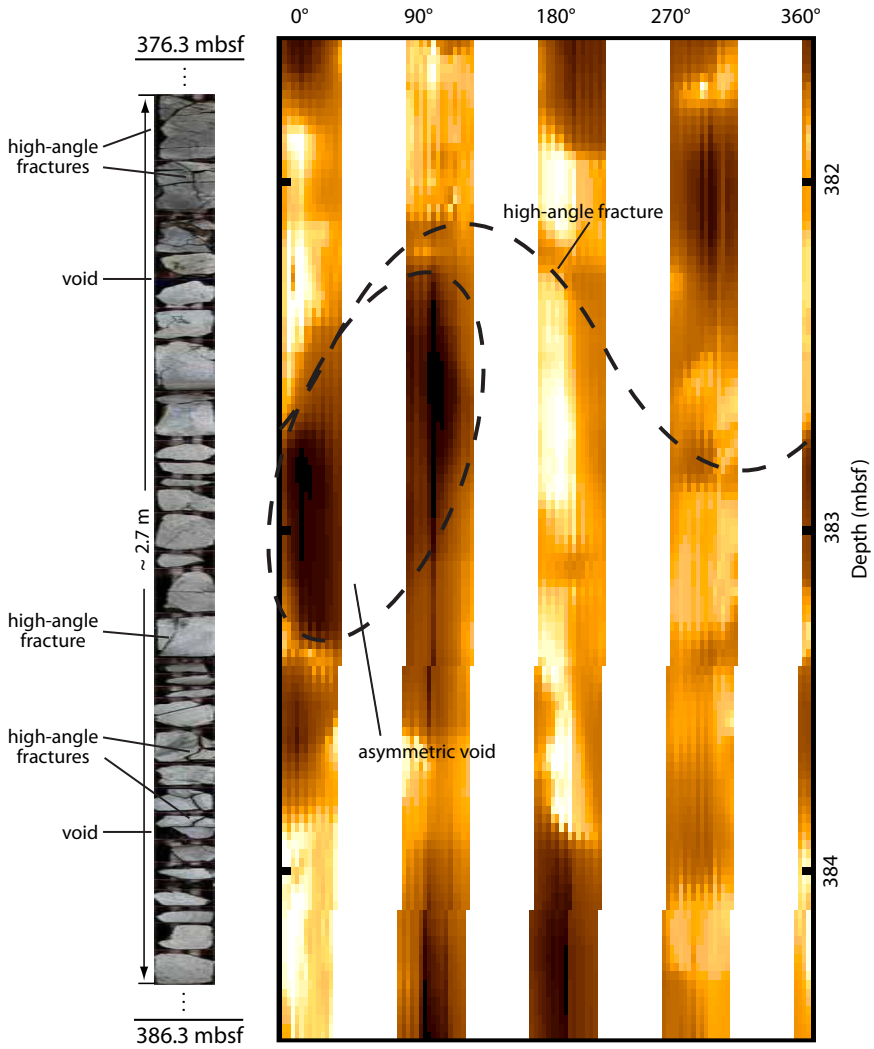

Fig. 3. Deep-sea basalt core and downhole image. *In situ* microresistivity image representing the interior circumference of the hole (42) over a 2.7-m interval at Site U1301. Massive flows and intact lavas have high resistivities and appear bright in the image; conductive features such as seawater-filled voids, fractures, and contacts between pillow lavas and flows appear dark and reflect the porous, asymmetric structure of basalt basement. Massive flows with high-angle fractures are also observed in a 2.7-m core recovered between 376 and 386 m below the seafloor. For improved illustration, the horizontal/vertical exaggeration is 3:1 for the core image and 2:3 for the downhole image. Core and downhole data come from the Integrated Ocean Drilling Program database (www.iodp.org/).

of Vancouver Island, Oregon, and Washington, are known to contain highly fractured, channelized, and highly porous (10–15%) basalt basement that is widely blanketed by impermeable fine-grained turbidities and hemipelagic clay sediments (31). From drilling studies, the basalts are known to comprise both pillow lavas and massive flows containing plagioclase, olivine, and clinopyroxene, with slight to moderate (5–25%) alteration minerals that fill veins (32). Clays, mostly saponite, are identified in 98% of the veins, and calcite is present as vein-filling material as well. Recently drilled on the Juan de Fuca plate, Site U1301 illustrates the variability of porosity with depth in basalt basement as computed by using *in situ* geophysical logs (Fig. 2). Measurements on recovered core samples do not reflect the fracture porosity and void space present within the basement. In Fig. 2, we observe that the resistivity-derived porosity is most consistent with results from recovered core samples in massive flows (2–9%), and measures as high as 20% in pillow lavas and fractured zones. Neutron- and density-derived estimates are consistently lower within massive flows than in fractured intervals, but erroneously overestimate porosity because of the enlarged volume of the hole. These data indicate that massive flows are bounded by several 5- to 10-m-thick fractured intervals over 230 m of basalt basement. Fig. 3 illustrates a 2.7-m interval of pillow basalt at Site U1301, acquired by using an *in situ* circumferential microresistivity device where the hole conditions allowed for sufficient wall contact. Nodules of massive basalt, intact pillows, and flow layers are apparent in the image as resistive (bright) areas, whereas seawater-filled voids, fractures, and contacts are conductive (dark). Although core recovery over this interval was 34% and its depth can only be approximated to within ±3 m, numerous core breaks, void spaces, and high-angle fractures observed in the core also reflect the fractured, porous, and asymmetric structure of basalt basement drilled at this site (Fig. 3 *Left*). Interconnectivity of such basement fractures and porous structures would yield high bulk permeability values over wide areas; pilot injection and tracer permeability tests are needed to establish the extent of permeable basement in the ocean crust.

In situ basement temperatures of 62–64°C measured in adjoining drill holes across the Juan de Fuca plate are nearly isothermal, suggesting vigorous hydrothermal circulation (33). Bulk permeability estimates in the shallow basement range from

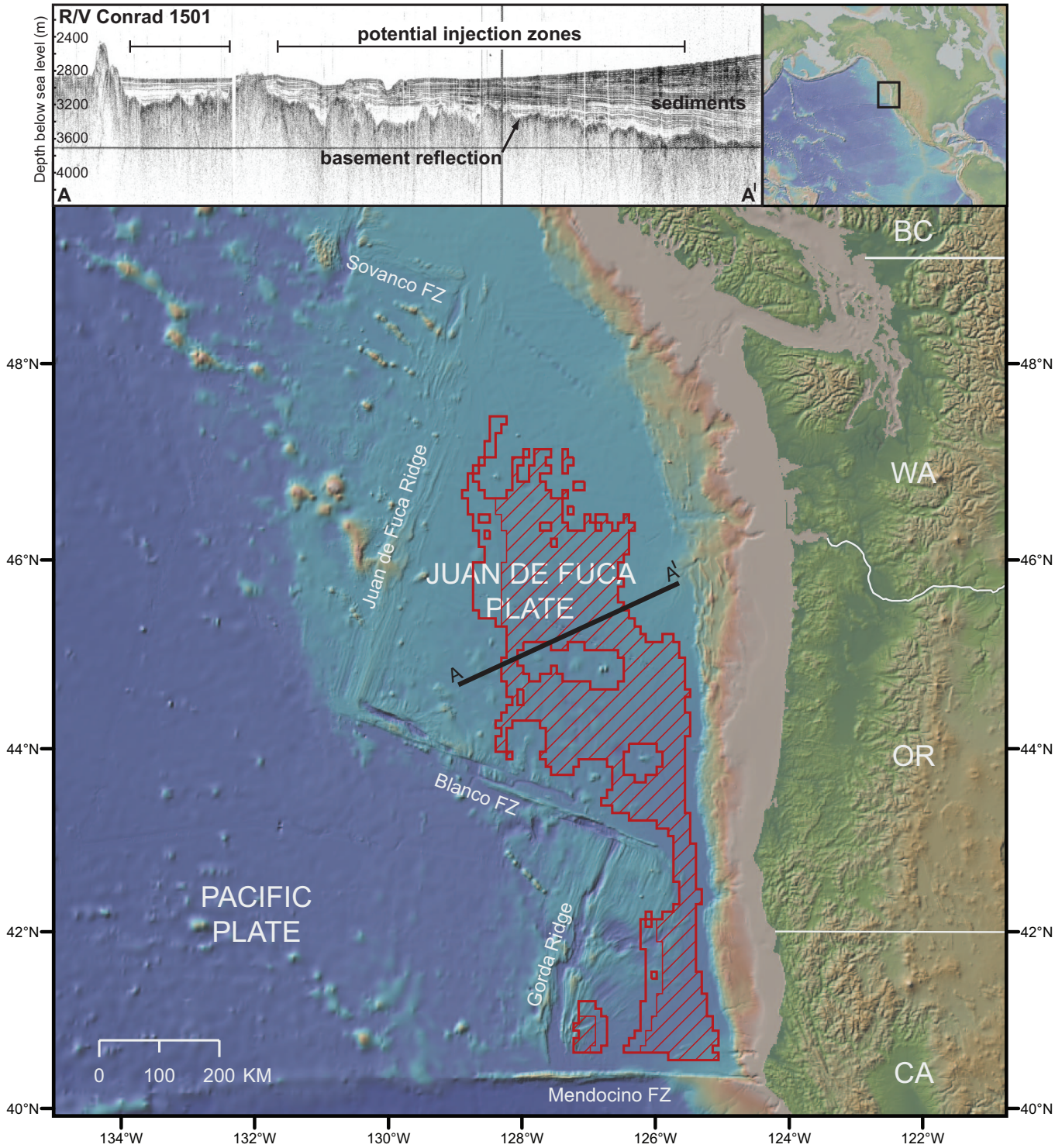

Fig. 4. Deep-sea basalt region for CO_2 sequestration. Red outline shows the region where water depths are ≥2,700 m and sediment thickness is ≥200 m, covering an area of 78,000 km^2. Hatched region shows the decrease in area having ≥300 m sediment cover, resulting in a total area of 68,000 km^2. The region excludes seamounts with >100 m of topographic relief and areas close to the surrounding plate boundaries and the base of the continental shelf. Heavy black line indicates the location of a single-channel seismic profile through potential CO_2 injection zones (R/V Conrad line 1501, *Inset Top Left*). Sediment thickness data comes from a digital database compiled by the National Geophysical Data Center (44), with a 5 arc-minute by 5 arc-minute grid spacing, providing a minimum value for the total thickness of sediment. The Marine Geoscience Data System (http://www.marine-geo.org/) provides ocean bathymetry, merging multibeam bathymetry with regional lower-resolution compilations, predicted topography from Smith and Sandwell (45), as well as land topography from the NASA Space Shuttle Radar Topography Mission (http://srtm.usgs.gov).

10^{-9} to 10^{-13} m^2, in general, decreasing with depth (31). *In situ* temperatures and isotopic C^{14} age dates show that the basement pore waters are younger (≈4,300 years) at sites more distant from the ridge axis and flow at rates of 1–5 m/year (34). Considering diffusive losses, however, fluid velocities within permeable basement may be considerably higher than rates

derived from pore water chemistry (35). Recent cross-hole flow experiments in basalt basement estimate lateral bulk permeability to be 10^{-12} m^2, an order of magnitude lower than borehole-scale packer tests, which has been attributed to permeability anisotropy within the upper basement (36). Surface heat flow surveys identify a recharge site with depressed isotherms at a distant seamount on the Juan de Fuca plate, which implies a lateral bulk permeability of 10^{-10} to 10^{-12} m^2 in the basement along that flow path (37). Based on coupled thermal modeling, high-permeability ($\approx 10^{-9}$ to 10^{-10} m^2) channels with lateral flow rates of up to 40 m/year match the observed thermal and flow regimes and require just one-sixth of the ocean crust to be permeable to 600 m thickness (35, 38). Other drilling results have observed active 1- to 10-m-thick fluid aquifers within basalt basement, persisting to 600 m thickness (39, 40). Fluid chemistry analyses indicate that the overlying sediments effectively seal hydrothermal flow within the basement and that the residence time for basement fluids is sufficiently long for them to chemically react with altered basalt (41). Evidenced by these studies, *in situ* fluids circulate laterally within the ocean crust on the Juan de Fuca plate, react with vast volumes of basalt, and remain trapped below ocean sediment for long periods of time.

Potential Storage Volume

CO_2 injected into deep-sea basalt is a supercritical fluid, and may be mixed with and dispersed into the aquifer through turbulent mixing processes and displacement of the aquifer fluid. Fluid-rock chemical reactions will proceed rapidly on surfaces of fractured basalt and within pore spaces. For selected injection targets in basement reservoirs that exist below $\approx$2,700 m water depth and are covered by 200 m or more of sediment, both gravitational and stratigraphic trapping will occur as well as geochemical trapping. Fig. 4 illustrates the extent of the region on the Juan de Fuca plate that satisfies these bathymetric and sediment thickness constraints. We restrict the region to avoid natural fluid inflow/outflow areas within 20 km of seamounts, the Juan de Fuca ridge, the Cascadia trench, and the Blanco and Mendocino fracture zones. By using the high, model-constrained estimate of 40 m/year lateral flow rate in the shallow crust, this restriction sets a 500-year buffer around potential natural outflow zones on the Juan de Fuca plate to further protect against the possibility of long-term CO_2 leakage to the seafloor. We compute $\approx$78,000 km^2 in the region that meet these depth and geologic conditions. Assuming that a channel system dominates the permeability over one-sixth of the upper 600 m of basement (38), we estimate that this area contains 7,800 km^3 of highly permeable basalt. Given an average channel porosity of 10% (33, 38), we can calculate that 780 km^3 of potential pore volume will be available for CO_2 storage. If liquefied CO_2 is injected to fill this volume, and it remains in liquid form (CO_2 density $\approx$1 g/cm^3, or 0.27 g C/cm^3), the total storage capacity for injected CO_2 in this area is 208 Gt of carbon. If all of the CO_2 becomes fixed as carbonate ($CaCO_3$ density $\approx$2.7 g/cm^3, or 0.36 g C/cm^3), with complete acid neutralization reaction with basalt, this reservoir could hold $\approx$250 Gt of carbon. Increasing the sediment cover to $\geq$300 m thickness will decrease the area by 12% to 68,500 km^2 and the volume to 685 km^3 for this region. For example, at the current annual emission rate of 1.7 Gt of carbon per year by the United States (5), the basement on the Juan de Fuca plate alone would provide sufficient CO_2 sequestration capacity for 122–147 years, depending on whether all of the injected CO_2 converts to carbonate. Given its proximity to the U.S. west coast, however, a more realistic scenario may be to assess the Juan de Fuca reservoir as a sequestration option for CO_2 sources from western states, via pipeline transport. Of course, if this becomes technologically and economically feasible, the reservoir would fill over a considerably longer time than estimated for U.S. emissions from the entire country.

Discussion

The injection of CO_2 in deep-sea basalt offers critical advantages for sequestration that warrant pressing investigation. The injection of CO_2 into deep-sea basalt facilitates the formation of stable carbonates retarding the return of CO_2 to the atmosphere, provides sufficient depth for denser CO_2 liquid to sink, blocks upward migration of acidified basement fluids with an impermeable sediment cover, and forms stable hydrate if CO_2 accidentally escapes to shallower depths with cooler water temperatures. Further research for CO_2 sequestration in deep-sea basalt is essential and should aim toward a pilot injection study. Important topics for ongoing research include *in situ* reaction rates for dissolution of injected CO_2, carbonate precipitation rates and the resulting rates of change in permeability, competing and augmenting effects of alteration, and site-specific hydrological testing. Only through further scientific investigation of these *in situ* effects can we confidently determine the viability of deep-sea basalt reservoirs such as the Juan de Fuca plate, which offers a geological option with potentially enormous capacity and highly secure CO_2 storage. Once established with more extensive scientific study, the ensuing technical challenges of building the infrastructure to use this reservoir, such as pipeline transport, subsea maintenance, and post-injection monitoring systems, can be quantified and evaluated, and their costs can be estimated. The critical step toward these goals is to improve our scientific understanding of the *in situ* processes that will occur after CO_2 injection in deep-sea basalt; the proximity of possible study locations on the Juan de Fuca plate to U.S. ports, potential sources of CO_2, and previous deep-sea studies make this area a wise choice for a pilot investigation.

ACKNOWLEDGMENTS. We thank T. Liu for assistance with preparation of Figs. 2 and 3.This work was supported by the Lamont-Doherty Earth Observatory and the Earth Institute at Columbia University.

1. Hoffert MI, *et al.* (2002) Advanced technology paths to global climate stability: Energy for a greenhouse planet. *Science* 298:981–987.
2. Lackner KS (2003) A guide to CO_2 sequestration. *Science* 300:1677–1678.
3. Pacala S, Socolow R (2004) Stabilization wedges: Solving the climate problem for the next 50 years with current technologies. *Science* 305:968–971.
4. Lackner KS, Sachs JD (2005) A robust strategy for sustainable energy use. *Brookings Papers on Economic Activity* 2:215–284.
5. Working Group III of the Intergovernmental Panel on Climate Change (2005) *IPCC Special Report on Carbon Dioxide Capture and Storage*, eds Metz B, Davidson O, de Coninck HC, Loos M, Meyer LA (Cambridge Univ Press, New York).
6. Bachu S, Gunter WD, Perkins EH (1994) Aquifer disposal of CO_2 hydrodynamic and mineral trapping. *Energy Conversion Manag* 35:269–279.
7. Bergman PD, Winter EM (1995) Disposal of carbon dioxide in aquifers in the US. *Energy Conversion Manag* 36:523–526.
8. Hitchon B (1996) *Aquifer Disposal of Carbon Dioxide: Hydrodynamic and Mineral Trapping—Proof of Concept*, ed Hitchon B (Geoscience Publishing Ltd., Alberta).
9. Holloway S (2001) Storage of fossil fuel-derived carbon dioxide beneath the surface of the Earth. *Ann Rev Energy Environ* 26:145–166.
10. Jessen K, Kovscek AR, Orr FM, Jr (2005) Increasing CO_2 storage in oil recovery. *Energy Conversion Manag* 46:293–311.
11. Hawkins DG (2004) No exit: Thinking about leakage from geologic carbon storage sites. *Energy* 29:1571–1578.
12. Rochelle CA, Czernichowski-Lauriol I, Milodowski AE (2004) The impact of chemical reactions on CO_2 storage in geological formations: A brief review. *Geological Storage of Carbon Dioxide*, eds Baines SJ, Worden RH (Geological Society of London, London), Special Publication 233, pp 87–106.
13. Gunter WD, Bachu S, Benson S (2004) The role of hydrogeological and geochemical trapping in sedimentary basins for secure geological storage of carbon dioxide. *Geological Storage of Carbon Dioxide*, eds Baines SJ, Worden RH (Geological Society of London, London), Special Publication 233, pp 129–145.
14. Barnes I, O'Neil JR (1969) The relationship between fluids in some fresh Alpine-type ultramafics and possible modern serpentinization, Western United States. *Geol Soc Am Bull* 80:1947–1960.
15. Neal C, Stanger G (1985) Past and present serpentinization of ultramafic rocks: An example from the Semail ophiolite nappe of northern Oman. *The Chemistry of Weathering*, ed Drever JI (D. Reidel Publishing Co., Dordrecht, The Netherlands), pp 249–275.

16. Kelley DS, *et al.* (2001) An off-axis hydrothermal vent field near the Mid-Atlantic Ridge at 30° N. *Nature* 412:145–149.
17. Seifritz W (1990) CO_2 disposal by means of silicates. *Nature* 345:486.
18. Goldberg D (1999) CO_2 sequestration beneath the seafloor: Evaluating the in situ properties of natural hydrate-bearing sediments and oceanic basalt crust. *Int J Soc Mater Eng* 7:11–16.
19. Gunter WD, Perkins EH (1993) Aquifer disposal of CO_2-rich gases: Reaction design for added capacity. *Energy Conversion Manag* 34:9–11.
20. Baines SJ, Worden RH (2004) The long-term fate of CO_2 in the subsurface: Natural analogues for CO_2 storage. *Geological Storage of Carbon Dioxide*, eds Baines SJ, Worden RH (Geological Society of London, London), Special Publication 233, pp 59–85.
21. Takahashi T, Goldberg D, Mutter JC (2000) Secure, long-term sequestration of CO_2 in deep saline aquifers associated with oceanic and continental basaltic rocks. *Proceedings of the SRI International Symposium, Deep Sea & CO_2* (The Ship Research Institute, Mitaka), pp 4-1-1–4-1-7.
22. McGrail BP, *et al.* (2006) Potential for carbon dioxide sequestration in flood basalts. *J Geophys Res* 111: B12201, 10.1029/2005JB004169.
23. Kaszuba JP, Williams LL, Janecky DR, Hollis WK, Tsimpangogiannis IN (2006) Immicible CO_2-H_2O fluid in the shallow crust. *Geochem Geophys Geosyst* 7:Q10003.
24. Jarrard RD, Abrams LJ, Pockalny R, Larson RL, Hirono T (2003) Physical properties of upper oceanic crust: Ocean Drilling Program Hole 801C and the waning of hydrothermal circulation. *J Geophys Res B* 108:2188.
25. Matter JM, Takahashi T, Goldberg D (2007) Experimental evaluation of in situ CO_2-water-rock reactions during CO_2 injection in basaltic rocks: Implications for geological CO_2 sequestration. *Geochem Geophys Geosyst* 8:Q02001.
26. Brewer PG, Friederich G, Peltzer E, Orr FM, Jr (1999) Direct experiments on the ocean disposal of fossil fuel CO_2. *Science* 284:943–945.
27. Koide H, *et al.* (1997) Deep sub-seabed disposal of CO_2—The most protective storage. *Energy Conversion Manag* 38:S253–S258.
28. House K, Schrag D, Harvey C, Lackner K (2006) Permanent carbon dioxide storage in deep-sea sediments. *Proc Nat Acad Sci USA* 103:12291–12295.
29. Levine J, Matter J, Goldberg D, Cook A, Lackner K (2007) Gravitational trapping of carbon dioxide in deep sea sediments: Permeability, buoyancy, and geomechanical analysis. *Geophys Res Lett* 34: L24703.
30. Fisher AT (1998) Permeability within basaltic oceanic crust. *Rev Geophys* 36:143–182.
31. Davis EE, Becker K (1998) Borehole observatories record driving forces for hydrothermal circulation in young oceanic crust. *EOS Trans Am Geophys Union* 79:369–378.
32. Fisher AT, Urabe T, Klaus A, IODP Expedition 301 Scientists (November 1, 2005) IODP Expedition 301 installs three borehole crustal observatories, prepares for 3-dimensional cross-hole experiments in the northeastern Pacific Ocean. *Scientific Drilling*, 10.2204/iodp.sd. 1.01.
33. Fisher AT, Becker K, Davis EE (1997) The permeability of young ocean crust east of the Juan de Fuca Ridge as determined using borehole thermal measurements. *Geophys Res Lett* 24:1311–1314.
34. Elderfield H, Wheat CG, Mottl MJ, Monnin C, Spiro B (1999) Fluid and geochemical transport through oceanic crust: A transect across the eastern flank of the Juan de Fuca Ridge. *Earth Planet Sci Lett* 172:151–165.
35. Stein J, Fisher AT (2003) Observations and models of lateral hydrothermal circulation and a young ridge flank: Numerical evaluation of thermal and chemical constraints. *Geochem Geophys Geosyst* 2:1026.
36. Fisher AT, Davis EE, Becker K (May 6, 2008) Borehole-to-borehole hydrologic response across 2.4 km in the upper oceanic crust: Implications for crustal-scale properties. *J Geophys Res*, 10.1029/2007JB005447.
37. Fisher AT, *et al.* (2003) Hydrothermal recharge and discharge across 50 km guided by seamounts on a young ridge flank. *Nature* 421:618–621.
38. Spinelli GA, Fisher AT (2004) Hydrothermal circulation within topographically rough basaltic basement on the Juan de Fuca Ridge flank. *Geochem Geophys Geosyst* 5:Q02001.
39. Wheat CG, Mottl MJ (2000) Composition of pore and spring waters from Baby Bare: Global implications of geochemical fluxes from a ridge flank hydrothermal system. *Geochim Cosmochim Acta* 64:629–642.
40. Bartetzko A, Pezard P, Goldberg D, Sun Y-F, Becker K (2001) Volcanic stratigraphy of DSDP/ODP Hole 395A: An interpretation using well-logging data. *Mar Geophys Res* 22:111–127.
41. Langseth MG, Becker K, von Herzen RP, Schulteiss P (1992) Heat and fluid through sediments on the western flank of the mid-Atlantic Ridge: A hydrogeological study of North Pond. *Geophys Res Lett* 19:517–520.
42. Goldberg D (1997) The role of downhole measurement in marine geology and geophysics. *Rev Geophys* 35:315–342.
43. Pezard PA (1990) Electrical properties of mid-ocean ridge basalt and implications for the structure of the upper oceanic crust in Hole 504B. *J Geophys Res* 95:9237–9264.
44. Divins DL (2007) *NGDC Total Sediment Thickness of the World's Oceans and Marginal Seas*. Available at: http://www.ngdc.noaa.gov/mgg/sedthick/sedthick.html. Accessed July, 2007.
45. Smith WHF, Sandwell DT (1997) Global seafloor topography from satellite altimetry and ship depth soundings. *Science* 277:1957–1962.